

HIGH-SPEED INLET RESEARCH PROGRAM AND SUPPORTING ANALYSIS

Robert E. Coltrin

SUMMARY

The technology challenges faced by the high-speed-inlet designer are discussed by describing the considerations that went into the design of the Mach 5 research inlet. It is shown that the emerging three-dimensional viscous computational fluid dynamics (CFD) flow codes, together with small-scale experiments, can be used to guide larger scale full inlet systems research. Then, in turn, the results of the large-scale research, if properly instrumented, can be used to validate or at least to calibrate the CFD codes.

INTRODUCTION

The design of a relatively simple-looking high-speed inlet is a complex task which presents many technology challenges. The inlet design process is much more difficult than the single development of an on-design configuration. The actual design is an iterative process in which inlet designers use their expertise to develop an overall system that will meet mission goals. The final design not only must represent a configuration that provides high performance at the design condition, but also must (1) function at off-design, (2) maintain acceptable shock stability for safety, (3) have minimum bleed requirement, (4) employ a reasonable variable geometry system, (5) allow boundary layer control systems and ducting, (6) provide required engine/combustor airflow, (7) be lightweight, (8) minimize drag, (9) provide for unstart and restart, (10) minimize sealing requirements, (11) incorporate additional systems for takeoff and landing and for control functions, and (12) be compatible with other engines and modules and with propulsion/airframe integration. Many designs that can provide very high internal performance for the design condition become unacceptable when the overall requirement is considered. Thus, in the past, most inlets have been designed by a few inlet experts using empirical methods to lay out the initial inlet lines, and then relying on their expertise based on years of experience (and a little "magic" where required) to accomplish the majority of the inlet design effort.

The state of the art of inlet design technology still relies on these same experts using their empirical methods. Method of characteristics codes are used to lay out the inviscid inlet lines at design conditions. Boundary-layer codes are then exercised, and the inviscid inlet lines are corrected for the boundary layer displacement thickness. However, there are new tools becoming available that the experts can use to help guide the inlet research once the lines are defined. These tools are the emerging three-dimensional viscous flow codes. This paper will use the Mach 5 inlet research program to show how these three-dimensional codes, together with small-scale research, can be used to guide the larger scale inlet systems research. The results of this large-scale

research, if properly instrumented, can then be used to validate or at least to calibrate the emerging CFD codes.

SYMBOLS

H_{c1}	height of cowl lip, m
M	Mach number
P_T/P_{REF}	local total pressure, ratioed to free-stream total pressure
X	horizontal length, m
Y	vertical length, m
α	angle of attack relative to first inlet ramp, deg

Subscripts:

I	local
∞	free stream

DISCUSSION

In the third paper of this session, Propulsion Challenges and Opportunities for High-Speed Transport Aircraft, Strack has described the importance of the inlet to high-speed aircraft (see also refs. 1 to 3), and has also described some of the important inlet characteristics as a function of cruise Mach number. Figure 1 shows some additional inlet features as a function of cruise speed. This is a simple generic plot of altitude versus Mach number with photographs of four typical research inlets. These photographs are placed on the plot in the altitude/Mach number arena in which they would be applicable.

In the low supersonic speed range up to Mach 2, inlets tend to be simple fixed-geometry configurations which employ entirely external compression. Normal shock inlets, like the HiMAT (Highly Maneuverable Aircraft Technology) research inlet (ref. 4) shown on the left, are often used. As discussed by Strack in this session, aircraft operating above Mach 2 must employ mixed compression in order to maintain high efficiency. Inlets in the Mach 2 to 4 range are usually pod mounted; therefore axisymmetric configurations are usually favored, but two-dimensional configurations can be considered. The second photograph from the left is of a variable-diameter centerbody (VDC) inlet that was studied as part of the Supersonic Cruise Aircraft Research Program in the 1970's (ref. 3). In the Mach 4 to 6 range, inlets tend to be more integrated into the airframe. Because of this integration, two-dimensional configurations are favored, but axisymmetric or half-axisymmetric configurations can be considered. A two-dimensional Mach 5 research inlet model is shown in the third photograph from the left. Inlets for Mach 6+ aircraft must be fully integrated into the airframe, and are therefore normally two-dimensional configurations.

A Langley Research Center inlet model which employs both ramp and sidewall compression is shown in the photograph at the right. This type of inlet was tested as part of the Langley scramjet program, which is described in the sixth paper of this session, Hypersonic Propulsion Research.

The remainder of this paper will describe the technique that was used for the design of the Mach 5 research inlet (third photograph from the left). This technique is generically representative of that used for any typical high-speed inlet design.

The Mach 5 inlet resulted from a program that was initiated in 1980 by NASA Langley, with NASA Lewis as a partner. The research study was a contractual program with Lockheed-California as prime contractor and Pratt & Whitney as subcontractor. The purpose of this study was to define an aircraft capable of sustained high-speed cruise in the Mach 5 arena, and specifically, to lay out the aircraft in enough detail so that the propulsion system and its integration with the aircraft could be defined. The final aircraft resulting from this study is shown in figure 2 and discussed in reference 5. The aircraft would employ four propulsion modules (two under each wing), with the inlets integrated into the wings but with the leading edge in the free stream. The propulsion system chosen for this aircraft is an over-under turbojet plus ramjet system with two-dimensional dual flow inlets and nozzles.

The various modes of operation for the over-under turbojet plus ramjet propulsion system are illustrated in figure 3. There are two flow paths through the propulsion system with a turbojet engine in the upper flow path and a ramjet engine in the lower flow path. The inlet and the nozzle each have a flow control diverter, which must be properly positioned at each point in the flight envelope to provide the required flow to each engine. At subsonic flight speeds, the turbojet engine only powers the aircraft, with cold flow through the ramjet duct. Near Mach 1 the ramjet is ignited, initially to help fill the large nozzle base area. Both systems are operating until the aircraft approaches Mach 3, where the ramjet engine then provides the total power. Between Mach 2.5 and 3 the turbojet spools down, and at Mach 3 the upper duct of the system is totally closed off. The turbojet engine is then in a sealed environment that can be cooled. From Mach 3 to cruise speed, the aircraft is powered by the ramjet engine only. Thus, this system takes maximum advantage of the turbojet engine in the low-speed range where it is most effective, and the ramjet engine in the high-speed range where it is most effective.

Once this propulsion system was defined, it was realized that there were many technology challenges associated with its design. One of the most challenging was the cruise performance and operating characteristics of the inlet. Could an inlet be designed that would provide sufficient performance, and how much boundary-layer bleed would be required to obtain this performance and maintain normal shock stability? This bleed question was crucial since excessive bleed drag could make the whole concept unacceptable. Therefore, the Mach 5 inlet program was initiated. The objective of the program was to design, analyze, build, and test a large-scale inlet for the cruise (ramjet) configuration and to define its performance and operating characteristics. Even though it was realized that the off-design operation and the transition from turbojet to ramjet operation posed many more challenges, it was decided that the make-or-break challenge was at cruise. If the cruise challenges could be met, the off-design challenges would be addressed in a later model.

The nozzle presents a similar set of design and off-design problems that would need to be addressed.

The aerodynamic design (cross section) of the Mach 5 inlet is shown in figure 4. The X- and Y-dimensions are nondimensionalized to the cowl lip height. Mach numbers in the various flow regions are shown for the cruise (Mach 5) condition. At cruise conditions, free-stream airflow is at an angle of 9° relative to the first ramp surface. The resulting first compression wedge of 9° and Mach 5 free-stream conditions gives a local Mach number of 4.1 on the first inlet wedge. The Mach conditions are successively reduced by additional wedges to obtain Mach 3.1 on the final external ramp surface. A cowl shock, additional distributed compression, and a terminal shock are employed for internal supersonic compression. The inlet was designed by using a conventional method-of-characteristics (MOC) approach to lay out the initial inlet inviscid lines. A boundary-layer code was then exercised, and the inviscid inlet lines were corrected for the boundary-layer displacement thickness. One of the main driving factors in the design was length minimization to reduce the weight as much as possible. In order to minimize length, the design calls for the cowl shock to be cancelled at the inlet shoulder, followed by a strong cowl generated compression fan. The design throat Mach number is 1.6 inviscidly, which is reduced to approximately 1.2 when boundary layer corrections are made. The design compression split is about 85 percent external (with four ramps) and 15 percent internal.

Once the inlet lines were established, the next step was to design the location and size of the boundary-layer bleed systems. This is where the inlet expert normally enters the picture. It is well known that on a two-dimensional basis, bleed will be required to control the oblique shock/boundary-layer and normal shock/boundary-layer interactions. But how much and where? And on a three-dimensional basis, how can the glancing sidewall shock/boundary-layer interactions and three-dimensional corner flow be controlled?

Figure 5 graphically demonstrates the glancing shock/boundary-layer interaction phenomena. The figure shows a simple 10° compression wedge installed across the entire width of the NASA Lewis 1- by 1-Foot Supersonic Wind Tunnel, which is operating at Mach 3. This wedge could represent the ramp of an inlet, and the tunnel wall the inlet sidewall. The oblique shock from this wedge interacts with the wall boundary layer, which has a thickness of approximately 1 in. The surface oil film shows flow patterns in the boundary layer. The oil flows indicate that the boundary layer on the wall is turned ahead of the oblique shock and follows the 27° shock angle rather than the 10° wedge angle that the free-stream flow follows. This boundary-layer flow is turned because of the pressure rise through the oblique shock wave, which is fed forward through the subsonic portion of the boundary layer. A large portion of the boundary-layer flow aft of the shock is also turned in a direction along the oblique shock angle. The low-energy boundary layer that has been turned ahead of the oblique shock migrates along the oblique shock wave and then interacts with the floor boundary layer, which could simulate an inlet cowl. This interaction produces a large three-dimensional glancing sidewall/corner shock wave interaction, which in an inlet would most likely cause an unstart.

Figure 6 shows a three-dimensional parabolized Navier-Stokes (PNS) solution for the configuration shown in figure 5. The code used for this analysis is PEPSIS, which is the supersonic code in the PEPSI series (described by

Abbott, Anderson, and Rice in session 3, and discussed in ref. 6). The graphics have been mechanized to show the surface velocity vectors, which should then be directly comparable to the experimental oil flow results of figure 5. By comparing the flow features of figure 5 with those of figure 6 (see also ref. 6), it can be seen that the PEPSIS results are qualitatively similar to the experimental results. These near-wall results gave us confidence to look at the PEPSIS results in midstream.

The lower portion of figure 7 shows the PEPSIS results for a very similar test case as was shown in figure 5. The results shown here are the analytical simulations (ref. 6) of an experiment conducted by Bogdonoff (refs. 7 to 9). Again, a simple 10° wedge spanned a wind tunnel operating at Mach 2.94. The wind tunnel wall was in the front plane of the paper and has been removed so that the flow patterns can be seen. In each plane cut across the flow path, the secondary velocity vectors in that plane are shown. The results are shown from the front wall to the centerline of the tunnel. Near the tunnel centerline, the wedge-generated oblique shock wave can be seen (horizontal line in the flow vectors) at each flow station. But as the shock wave glances along the sidewall boundary layer, a large interaction region can be seen. The velocity vectors indicate that the flow in this interaction region is along the ramp surface toward the sidewall, then up the sidewall forming a vortex. It can also be seen that, as in the case near the sidewall, the interaction region away from the sidewall extends well ahead of the oblique shock. The upper portion of figure 7 demonstrates what this glancing shock/sidewall interaction phenomenon means to an inlet. The boundary layer proceeding downstream on the sidewall is turned ahead of the oblique shock wave, and this low-energy flow migrates along the shock wave, eventually arriving at the inlet cowl lip. If the inlet employs multiple oblique shock waves, as does the Mach 5 inlet, this flow migration has a cumulative effect, with large regions of low-energy flow sweeping up the sidewall ready to be captured by the cowl.

The excellent comparison of the PEPSIS analysis with the Bogdonoff data (ref. 10), gave us confidence to next apply PEPSIS to the Mach 5 inlet. The result is shown in figure 8. The figure shows total pressure distributions on cross planes at several stations in the inlet aft of the cowl lip. Only half planes are shown, since flow is symmetrical. The cowl lip shock can be seen as a horizontal line in each cross plane near the inlet centerline. Near the sidewall it can be seen that the low energy flow that has swept up the sidewalls ahead of the cowl lip is captured by the cowl and continues to grow. At a station about halfway between the cowl lip and the ramp shoulder, the code predicts a very large flow separation.

Figure 9 shows a more detailed view of the last cross plane of figure 8. The figure shows the total pressure distribution for the entire cross section, and the secondary velocity vectors have been superimposed. The cowl oblique shock can be seen in midstream. The flow in the corner flows up the sidewall and across the cowl in vortex fashion. A separated zone is indicated. As can be seen, the flow within a relatively simple-looking two-dimensional inlet is highly three-dimensional. In fact, the only location in the cross plane where the flow may be nearly two-dimensional is along the vertical centerline. But even here potential flow problems are developing.

The midstream ramp boundary layer, which started at zero thickness at the leading edge of the ramp, is very thick at this station. If this boundary layer would be allowed to proceed down the inlet to where the cowl shock (or

later the normal shock) would interact with it, a separation would most likely occur. In order to analyze this phenomenon, which potentially could involve subsonic flow and separated zones, full Navier-Stokes (NS) codes must be employed.

A two-dimensional Navier-Stokes analysis of the Mach 5 inlet is shown in figure 10. This analysis was carried out by W. Rose and E. Perkins of Rose Engineering and Research, consultants to Lockheed on the Mach 5 project. The analytical code was developed by Kumar of the NASA Langley Research Center. The Mach number distribution for the no-bleed case shown on the left represents the area encompassed by the large (single cross-hatched) box in the inlet sketch at the top. The Y (vertical) axis has been expanded by 3 1/2 times that of the X (horizontal) axis. It can be seen that there is a massive separation on the ramp surface, most likely caused by the interaction of the cowl lip generated shock. This plot is for one instant in the time marching solution. Because of the separation, the inlet cannot swallow the required airflow, and the inlet is on its way to unstart. No started stable solution was obtained. The Mach contours on the right, with 17 percent bleed (4 percent near the ramp shoulder and 13 percent in the normal shock region) distributed through the inlet, represent the area in the inlet throat (double cross-hatched) region in the sketch. The bleed prevents the larger separation seen at the left. The cowl lip shock is not quite cancelled at the ramp shoulder, and normal shock has been stabilized in the inlet. This is a steady solution. These analyses indicate that the experimentalist will have a difficult task in providing a high-performance inlet while maintaining low inlet bleed.

These results from the PNS and NS codes have been used to locate and size bleed systems for the Mach 5 inlet and to locate instrumentation. An isometric sketch of the model to be tested in the NASA Lewis 10- by 10-Foot Supersonic Wind Tunnel is shown in figure 11. A good test model can often be more complex than the actual flight configuration, since in the research and development process many additional parameters are investigated to arrive at an optimum configuration. This is especially true if both steady state and the very important transient phenomena are to be investigated. The Mach 5 inlet is such a model, as it incorporates remotely variable ramp geometry, main duct mass-flow control, and 15 bleed exit plugs. The model is extensively instrumented with static pressure taps, total pressure rakes, translating flow angularity probes, and dynamic pressure transducers. It is a very large model, with an overall model length of about 20 ft. The cowl lip height is 16 in., with a capture width of 16 in. The acceleration plate is 100 in. wide.

The requirement for the acceleration plate is shown in figure 12. The Lewis 10- by 10-Foot Supersonic Wind Tunnel has a maximum Mach number capability of 3.5, and the inlet has a design of Mach 5. In order to overcome this tunnel Mach number deficiency, the inlet is mounted beneath the large accelerator plate or expansion plate. The plate is then operated at negative angle of attack, and by taking advantage of the resulting expansion fan, the correct Mach number of 4.1 is generated on the first ramp (fig. 4). This "accelerator plate" test technique duplicates the actual inlet internal flow conditions with the exception that the initial oblique shock (Mach 5 and 9° wedge) is not present. This oblique shock would lay just above the sideplate leading edges and just above the cowl lip so that no shock/boundary-layer interactions are lost. What is lost is the pressure reduction through this initial oblique shock. The data will be corrected for this total pressure loss.

Figure 13 shows two photographs of the Mach 5 inlet model. The model is made of stainless steel, except for the accelerator plate, which is aluminum. On the right, a side view of the inlet is shown with the sidewall removed to show the variable ramp mechanisms. A single, large pair of actuators raises and lowers all movable sections of the ramp simultaneously. The inlet duct is entirely two-dimensional, from leading edge to mass-flow control plug. All bleed regions are compartmented to prevent recirculation. Collapsible bellows are used to duct the compartmentalized ramp bleed through the ramp plenum.

Figure 14 demonstrates the impact of the PEPISIS analysis on the model instrumentation and bleed systems. As a result of the PEPISIS analysis indicating boundary-layer migration from sidewall shock/boundary-layer interactions, modifications were made to the original model design. The dark band on the sidewall indicates the location of bleed holes added to the sidewall. The plenum behind this bleed region is compartmented to avoid reverse bleed. This bleed will allow the low energy boundary layer to be bled off before it is captured by the cowl. The dark area on the cowl corners indicate the location of cowl bleed. This will permit the removal of the low energy flow once it has been captured by the cowl. Not shown is the extensive two-dimensional bleed regions that were added to the ramp and cowl surfaces as a result of the Kumar code results.

The large size of this inlet makes it adaptable to the installation of more instrumentation than is possible on small-scale models. Figure 14 indicates the additional instrumentation that was added on the forward ramp and sidewall to map the flow migration phenomena and to provide code validation data.

At present, the testing of this inlet is scheduled for the summer of 1988. However, a small-scale model of the inlet was tested in the NASA Lewis 1- by 1-Foot Supersonic Wind Tunnel, and some typical results are shown in figure 15. This model had capture dimensions of 1.6 by 1.6 in. and duplicated the large-scale inlet geometry back to the cowl lip and ramp shoulder. Aft of these stations, the inlet was opened up to allow inlet starting. The schlieren photo on the lower left is for design flow conditions, with the inlet accelerator plate at the negative angle of attack relative to free-stream conditions. The ramp tip is off the picture to the left, but the Mach line generated by the expansion plate can be seen in the upper left portion of the photograph. The dark horizontal line is the leading edge of the sideplates. (For this photograph the metal sideplates have been changed to plexiglass sideplates.) The oblique shock waves from the second, third, and fourth ramps, as well as the cowl shock, can be seen. The cowl shock hits ahead of the ramp shoulder, and the resulting reflection can be seen. The surface oil film photograph at the right is for an off-design Mach number (Mach 3 on the first ramp). For the condition shown in the photograph, the inlet was unstarted, as indicated by the ramp flow near the cowl lip station. Upstream of this location the sidewall boundary-layer flow migration that results from the boundary-layer/glancing shock interaction can be seen, as well as the almost vertical migration ahead of the terminal shock location. This kind of small-scale research gives us confidence that the acceleration plate test technique is valid, and that the flow migration patterns are about what the codes predicted.

The aerodynamic design approach used to reduce the weight of the Mach 5 inlet is to decrease the length over which the distributed cowl compression intersects the ramp surface. This is accomplished by increased curvature of

the cowl and results in a large pressure rise over a short distance on the ramp. These large pressure gradients with large approach boundary layers can result in separation. A simple experimental program was conducted to study ramp bleed configurations to control the interaction of the pressure gradient and boundary layer in this region. Figure 16 shows that for this test, the cowl was simulated by a contoured compression plate, and the ramp by the tunnel wall (photograph on the upper right in the figure). The tunnel wall incorporated a bleed plate in which various bleed patterns could be studied. A translating probe was used to survey the flow field. When no bleed was employed, the boundary layer separated as expected. The left figure shows that when a distributed porous bleed configuration was attempted, separation was still present. This was the result of recirculation of the high-pressure airflow in the aft part of the bleed plenum, reversing the flow in the forward part of the plenum. When the bleed plenum was compartmentalized, as shown on the right, the boundary layer was successfully controlled, and a healthy boundary layer exited this compression fan zone. Thus, a bleed pattern is in hand for use in the initial large-scale testing. Thus, maybe for the first time, three-dimensional PNS analysis, two-dimensional NS analysis, and small-scale research experiments have all been used to guide the design and test planning of a large-scale inlet system at high speed.

Figure 17 shows the benefits to be obtained from the Mach 5 inlet test program. The main goals of this test plan are (1) to determine overall inlet performance and bleed requirements, and (2) to provide data for code validation and for the development of inlet design codes. The validation goals, as shown in the left column, are to validate or at least to calibrate the codes that have been used to pre-analyze the inlet. The operational goals shown on the right are equally important but have not been covered in this paper. This test program will validate the overall use of the design approach described in this paper, as well as the acceleration plate test technique. The amount and location of required inlet bleed will be determined, together with the tradeoff between bleed and performance. The unstart/restart characteristics, as well as the control signals required to control the overall inlet, will also be determined.

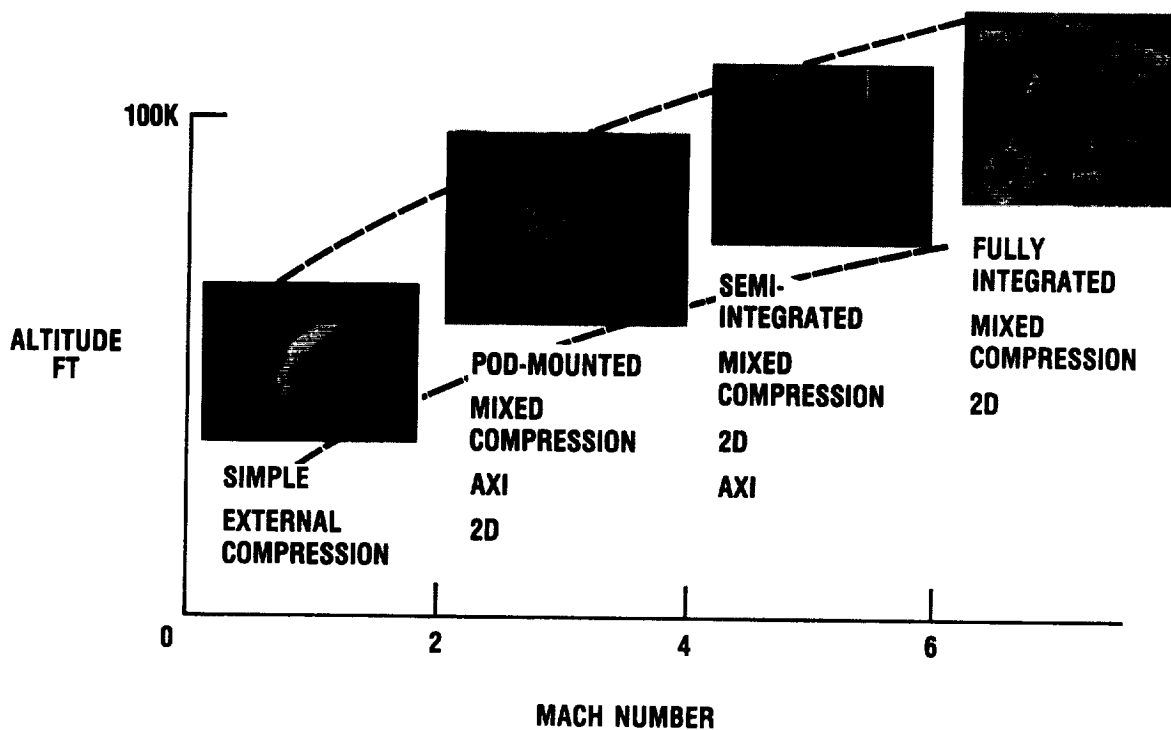
CONCLUDING REMARKS

The purpose of this paper was to describe the state-of-the-art inlet design and analysis techniques. These design techniques still rely on the traditional method-of-characteristics codes, with boundary-layer corrections. Thus, inlet experts are still the heart of the design process. However, the emerging three-dimensional viscous flow codes can now be used to guide the research in such areas as understanding local three-dimensional flow fields, placing and sizing bleed zones, and placing instrumentation. As the three-dimensional analytical codes become more validated and user friendly, they will become more and more a part of the design process. But the availability of a set of true three-dimensional viscous design codes that will generate the inlet surfaces on the basis of desired inlet flow properties is still a long way over the horizon. Even for the analytical codes, the inlet designer is continuously conceiving configurations that the existing codes cannot quite handle, and therefore they must be modified and revalidated. Thus, the few inlet experts will be required in the design loop for many years. The trick is to take maximum advantage of what each offers. The Mach 5 program may be the first large-scale high-speed inlet program to take maximum advantage of the inlet expert,

the tried and the true method-of-characteristics design code, the best available three-dimensional viscous flow codes, and small-scale experiments to guide the design and test planning of the inlet. We anxiously await the Mach 5 experimental results to determine the payoff of this design approach.

REFERENCES

1. Aircraft Propulsion. NASA SP-259, 1970.
2. Aeronautical Propulsion. NASA SP-381, 1975.
3. Aeropropulsion 1979. NASA CP-2092, 1979.
4. Neumann, H.E.; Povinelli, L.A.; and Coltrin, R.E.: An Analytical and Experimental Study of a Short S-Shaped Subsonic Diffuser of a Supersonic Inlet. AIAA Paper 80-0386, Jan. 1980 (NASA TM-81406).
5. Watts, J.D., et al.: Mach 5 Cruise Aircraft Research. Langley Symposium on Aerodynamics, NASA CP-2398, Vol. II, S.H. Stack, ed., 1985, pp. 285-304.
6. Anderson, B.H.: Three-Dimensional Viscous Design Methodology For Advanced Technology Aircraft Supersonic Inlet Systems. AIAA Paper 84-0194, Jan. 1984. (NASA TM-83558.)
7. Oskam, B.; Vas, I. E.; and Bogdonoff, S. M.: Mach 3 Oblique Shock Wave/Turbulent Boundary Layer Interactions in Three-Dimensions. AIAA Paper 76-336, July 1976.
8. Oskam, B.; Vas, I. E.; and Bogdonoff, S. M.: Oblique Shock Wave/Turbulent Boundary Layer Interactions in Three-Dimensions at Mach 3.0. AFFDL-TR-76-48-PT-I, June 1976.
9. Oskam, B.; Vas, I. E.; and Bogdonoff, S. M.: Oblique Shock Wave/Turbulent Boundary Layer Interactions in Three-Dimensions at Mach 3.0. AFFDL-TR-76-PT-II, Mar. 1978.
10. Anderson, B. H.; and Benson, T. J.: Numerical Solution to the Glancing Sidewall Oblique Shock Wave/Turbulent Boundary Layer Interaction in Three-Dimensions. AIAA Paper 83-0136, January 1983. (NASA TM-83056.)



CD-87-29935

Figure 1. - High-speed cruise inlets.



CD-87-28920

Figure 2. - Mach 5 cruise aircraft study.

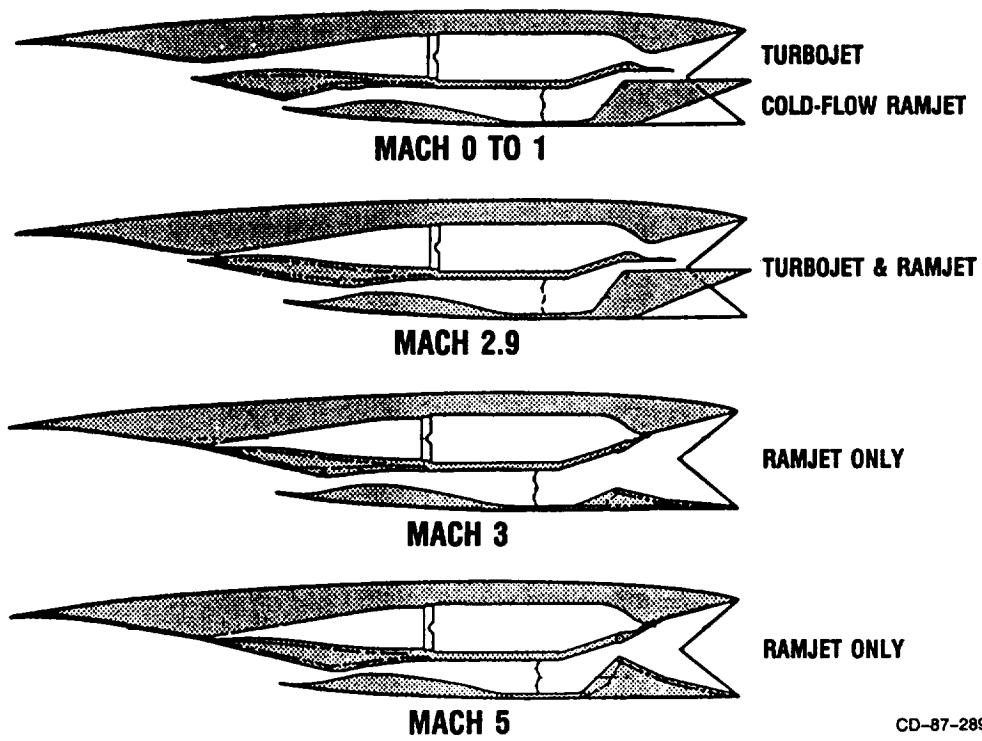


Figure 3. - Over-under turbojet/ramjet.

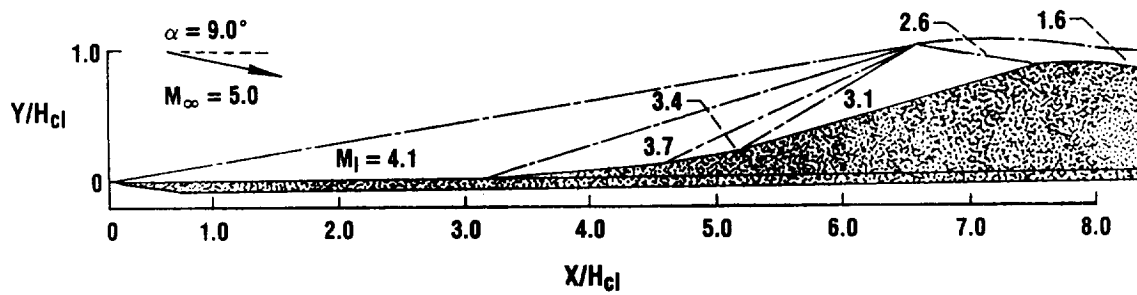
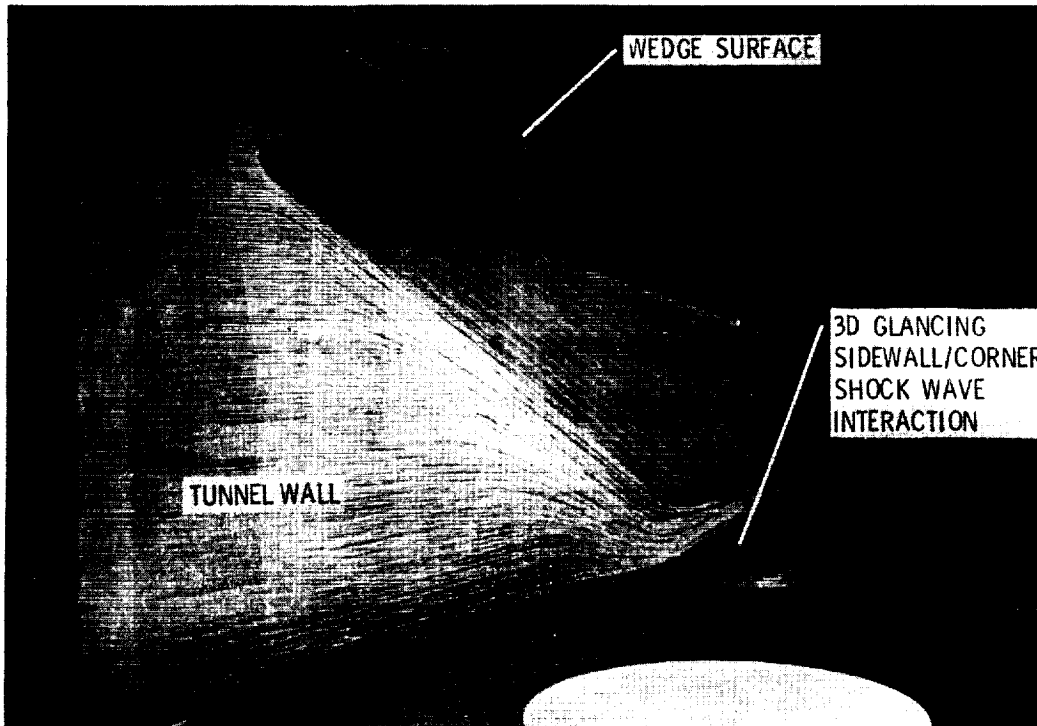
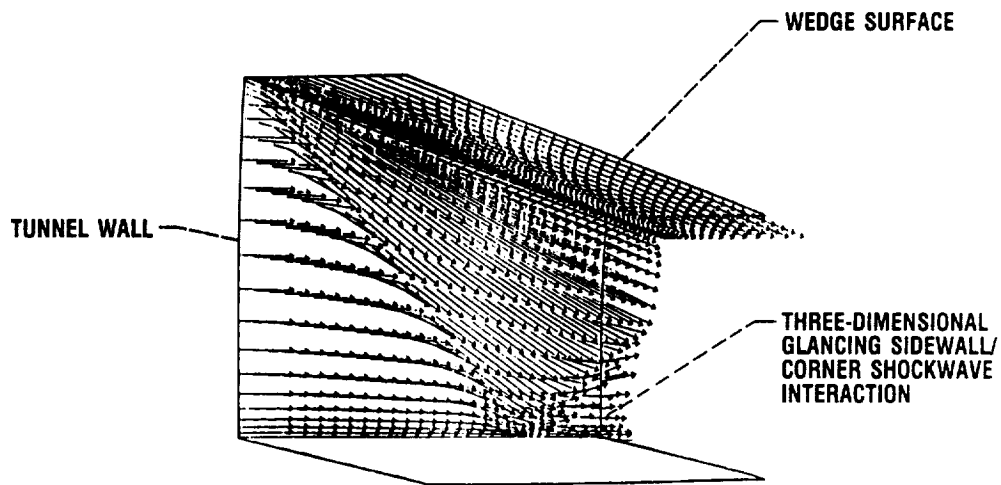


Figure 4. - Mach 5 inlet aerodynamic design configuration.



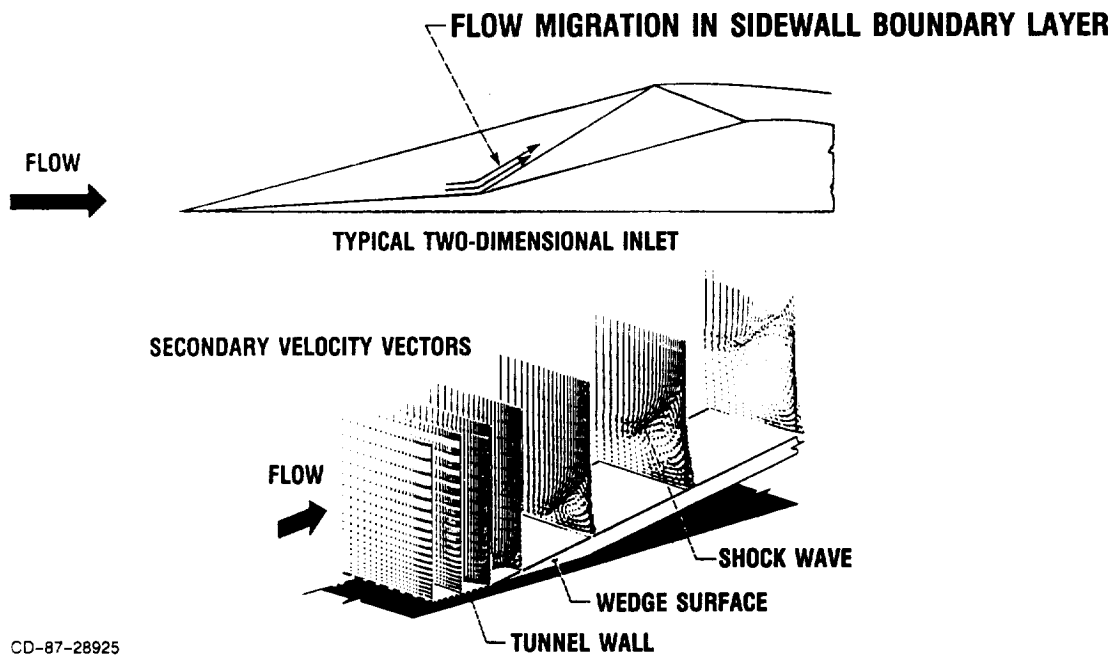
CD-87-28926

Figure 5. - Three-dimensional sidewall shock interaction (experimental surface oil film patterns).



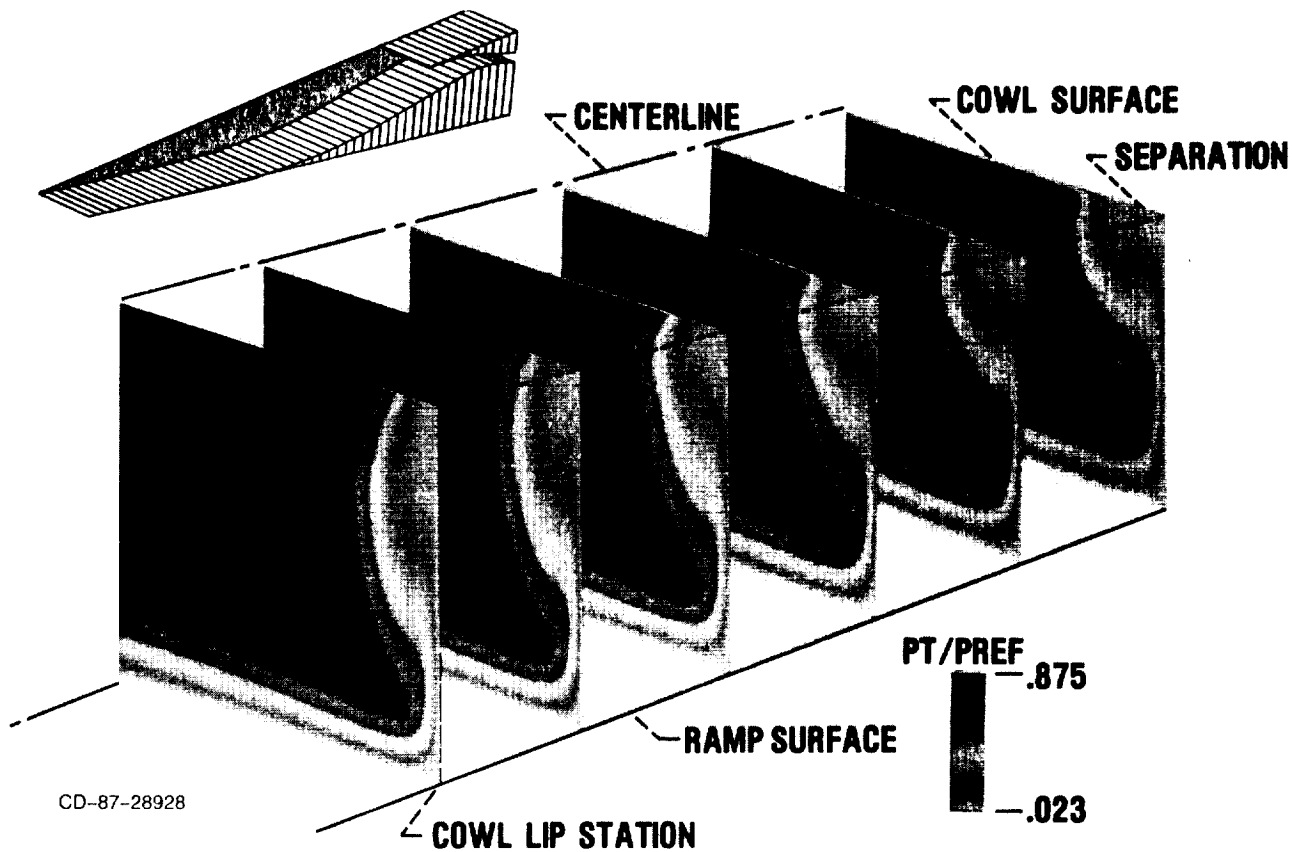
CD-87-28927

Figure 6. - Three-dimensional sidewall shock interaction (PEPSIS analytical surface oil film patterns).



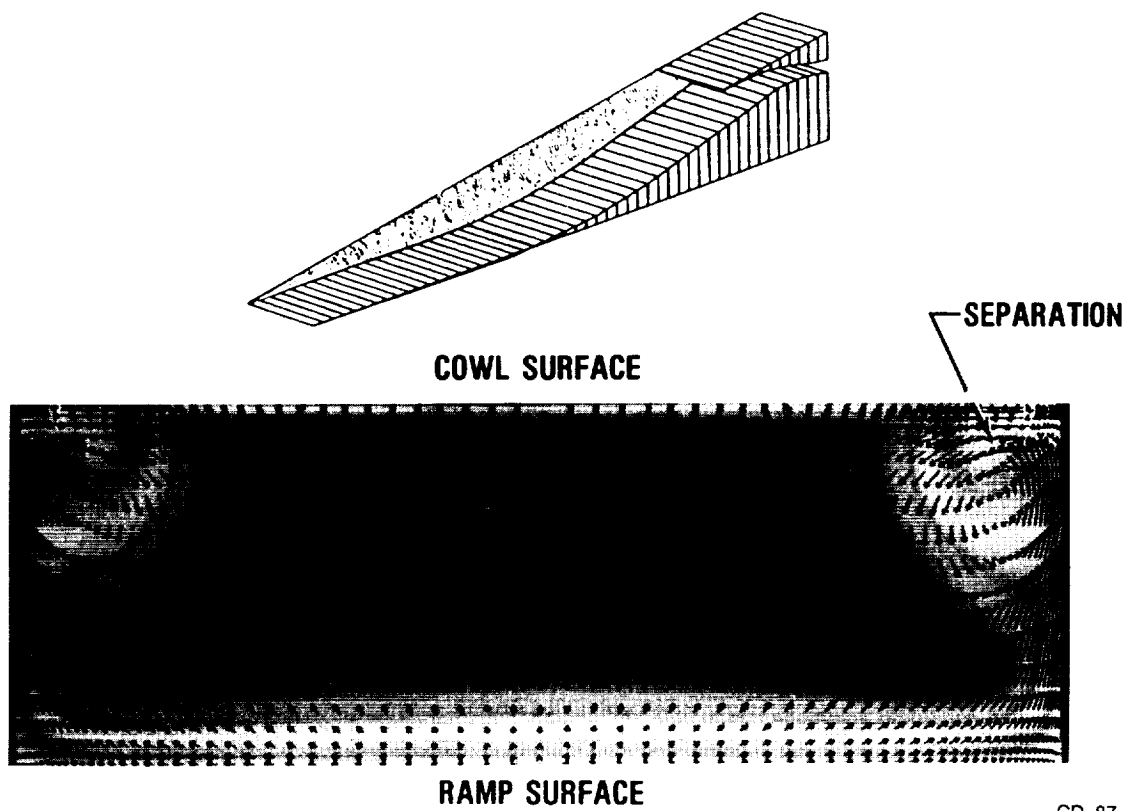
CD-87-28925

Figure 7. - Sidewall boundary-layer/glancing shock wave interaction - PEPSIS analysis.



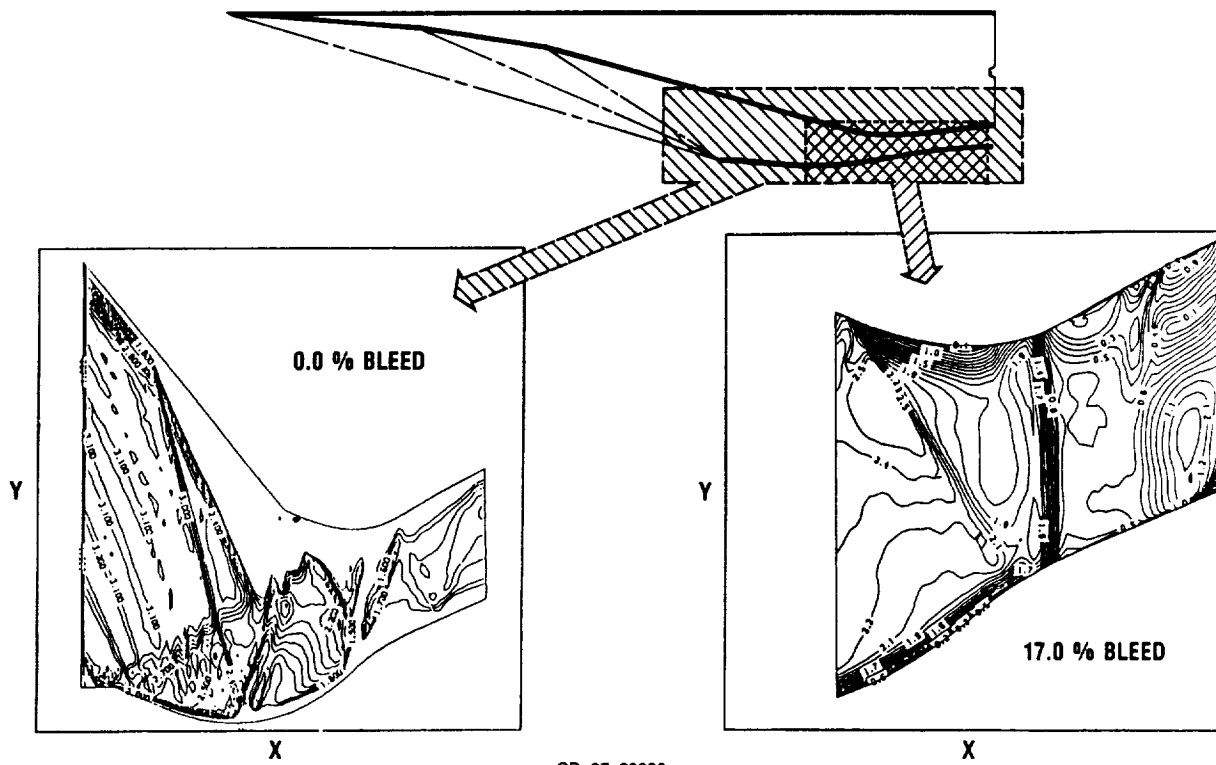
CD-87-28928

Figure 8. - PEPSIS analysis of Mach 5 inlet (total pressure distribution).



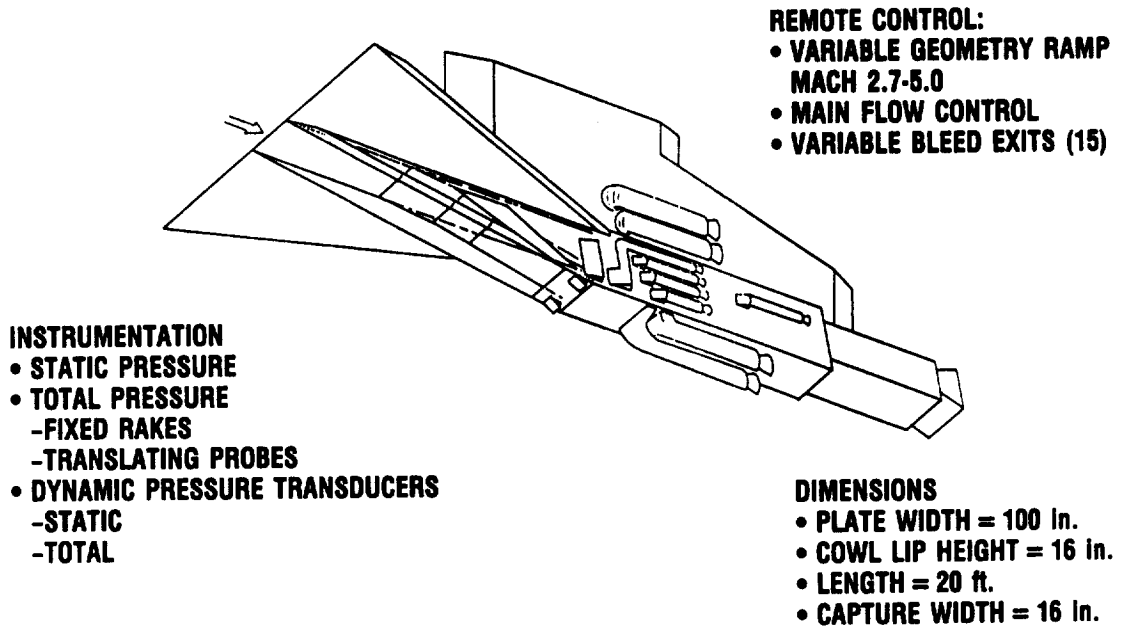
CD-87-28929

Figure 9. - Detailed PEPISIS analysis (total pressure).



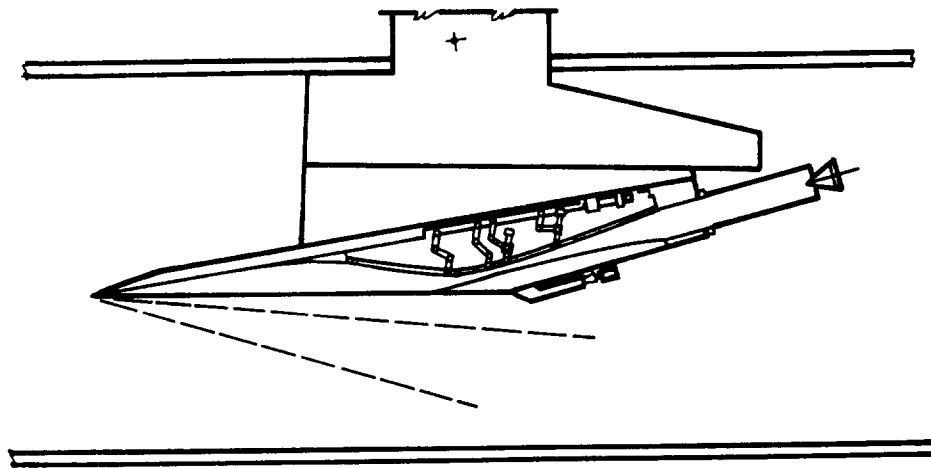
CD-87-28930

Figure 10. - Two-dimensional Kumar code analysis: Mach number contours.



CD-87-28933

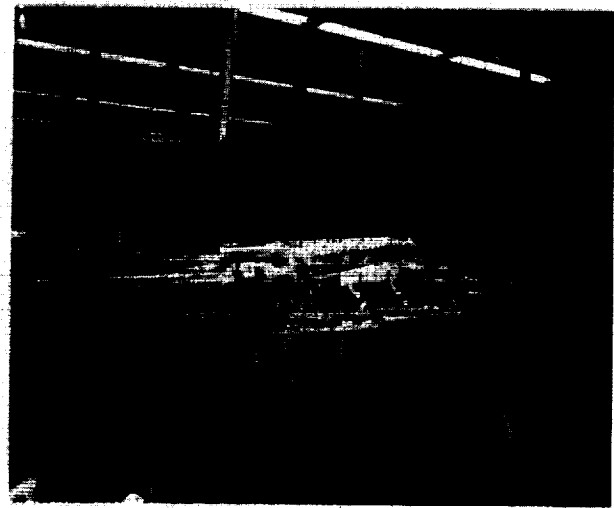
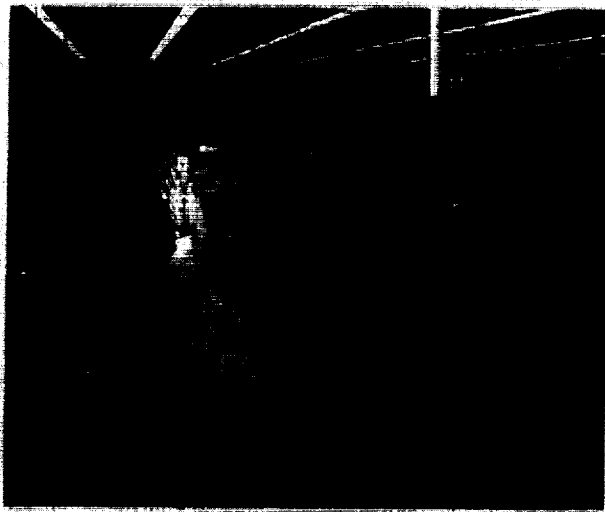
Figure 11. - Isometric sketch of Mach 5 inlet model.



TWO-DIMENSIONAL INLET INSTALLED IN 10 × 10 SWT

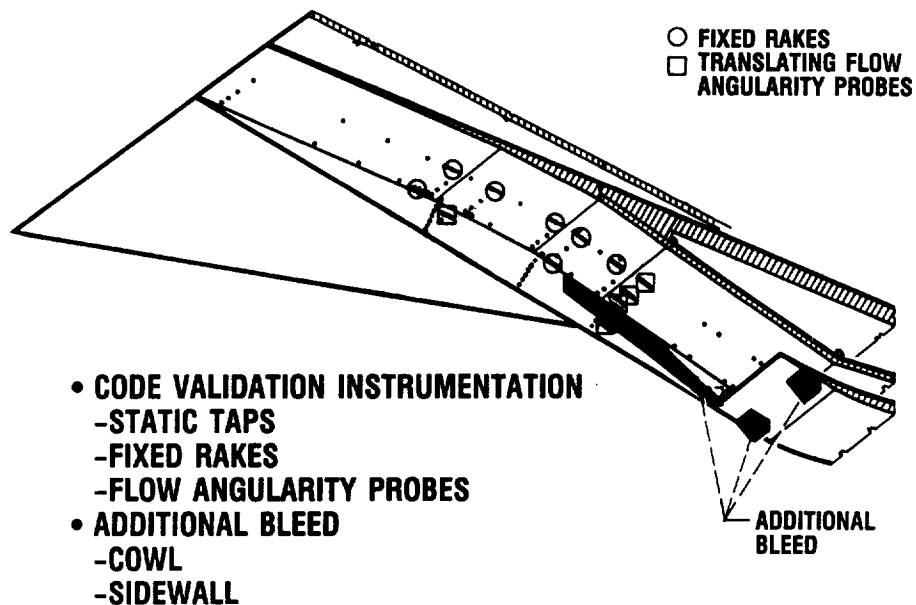
CD-87-28932

Figure 12. - Acceleration plate test technique.



CD-87-28934

Figure 13. - Mach 5 inlet test model.



CD-87-28935

Figure 14. - Effect of PEPISIS analysis on placement of model instrumentation and bleed systems.

TURBOJET AND RAMJET

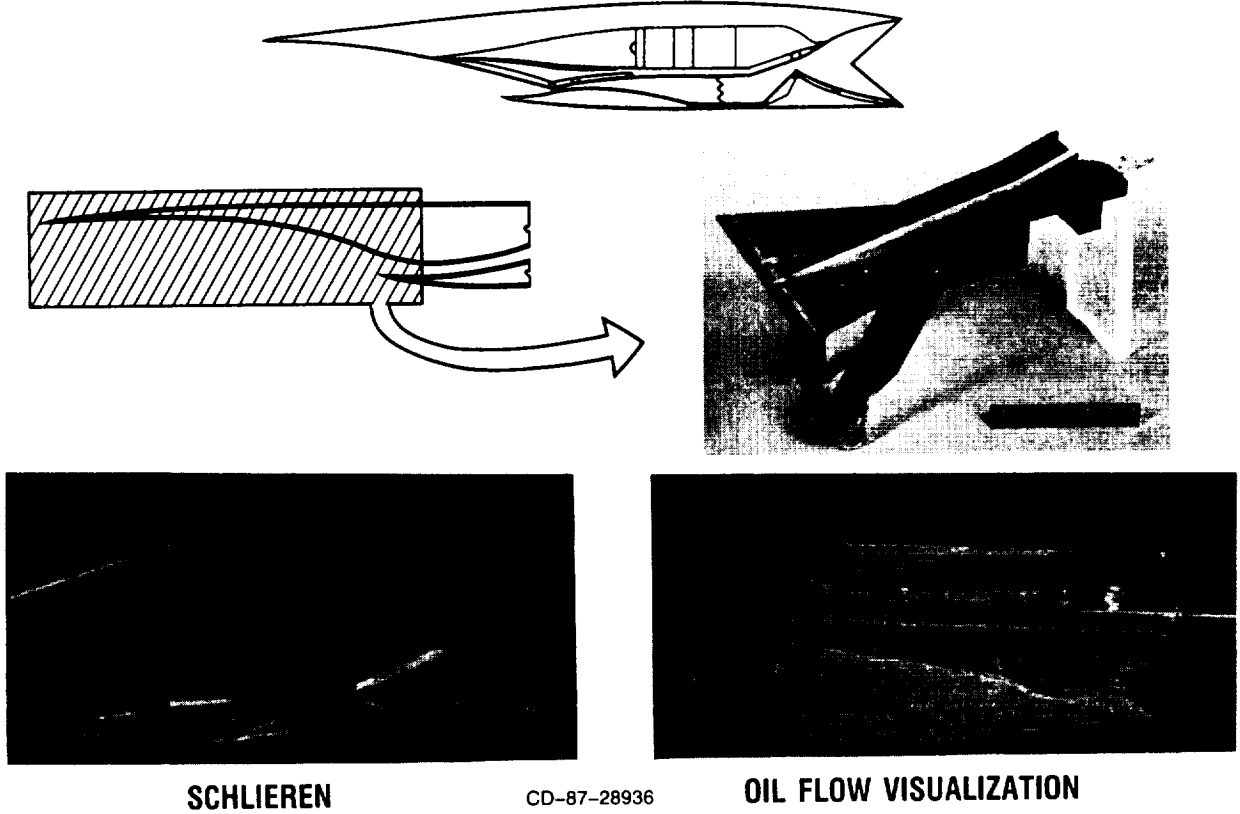
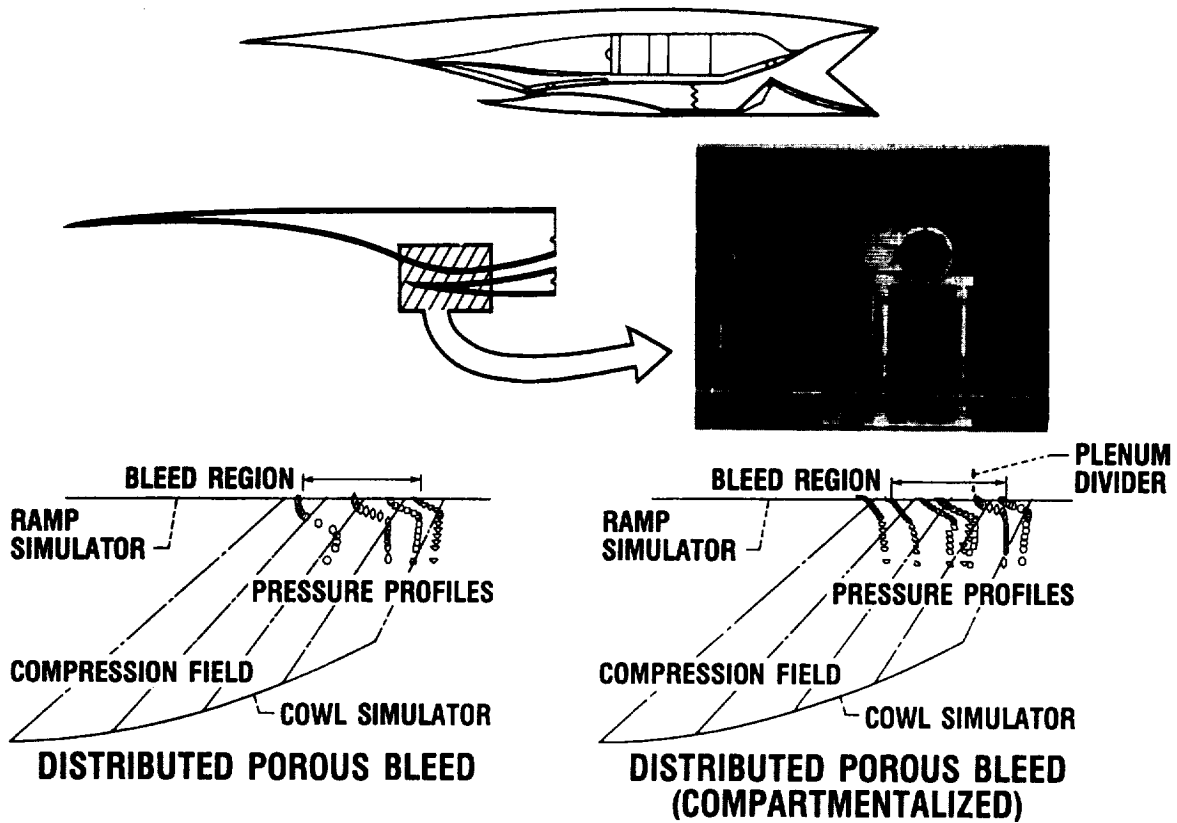


Figure 15. - Small-scale plate/ramp model (1- by 1-Foot Supersonic Wind Tunnel).



CD-87-28937

Figure 16. - Bleed control studies (1- by 1-Foot Supersonic Wind Tunnel).

PROVIDE FUNDAMENTAL AND DESIGN DATA FOR CODE VALIDATION

- GLANCING SIDEWALL SHOCK/ BOUNDARY LAYER INTERACTION
- THICK BOUNDARY LAYER/MULTIPLE AND OBLIQUE SHOCK INTERACTION
- THICK BOUNDARY LAYER/NORMAL SHOCK INTERACTION
- CORNER FLOW
- INLET DESIGN CODE DEVELOPMENT DATA

DETERMINE OVERALL INLET PERFORMANCE

- DESIGN AND OFF-DESIGN AERODYNAMIC CHARACTERISTICS
- BLEED REQUIREMENTS
- UNSTART/RESTART CHARACTERISTICS
- CONTROL DATA SIGNALS
- VERIFICATION OF INLET DESIGN TECHNIQUE
- VERIFICATION OF ACCELERATOR PLATE TEST TECHNIQUE

CD-87-28931

Figure 17. - Benefits to be obtained from inlet test program.